Distribution of Pb^{2+} Ions in PbF_2-Doped CaF_2 Crystals

M. Paraschiva, I. Nicoara*, M. Stef and O.M. Bunoiu
Department of Physics, West University of Timisoara, Bd. V. Parvan 4, Timisoara 300223, Romania

(Received May 11, 2009)

Calcium fluoride crystals doped with various concentrations of PbF_2 have been grown using the Bridgman technique. The optical absorption spectra reveal the characteristic UV absorption bands of the Pb^{2+} ions. The distribution of the Pb^{2+}-ions along four crystals has been investigated using the optical absorption method. Taking into account the relationship between the optical absorption coefficient and the concentration of the impurities in the samples, the effective segregation coefficient of the Pb^{2+} ions has been calculated. Our study shows that the effective segregation coefficient of the Pb^{2+} ions in CaF_2 host depends on the dopant concentration, and varies between 0.85 and 1.15, for 0.5 mol%PbF_2 and 3 mol%PbF_2-doped CaF_2, respectively.

PACS numbers: 42.70.Hj, 68.35.Dv, 78.20.Ci, 78.40.Ha, 81.10.Fq

1. Introduction

The study of optical properties of ns^2 ions in alkaline halide crystals is an old, well-studied domain [1]. There are few reports on optical properties of these ions in alkaline-earth fluorides; among the ns^2 ions, the Pb^{2+} ions are less investigated. Oboth et al. [2] studied the absorption and emission properties of Pb:CaF_2 crystals in vacuum UV spectral range. Various impurity-related color centers in alkaline-earth fluorides have been studied because these centers are laser-active in near IR. For example, the $Pb^{+}(1)$ centers in alkaline-earth fluorides have analogous properties to $Tl^{0}(1)$ center in alkali halides and are expected to act as laser-active centers [3, 4]. Babin et al. [5] studied the influence of Pb^{2+} ions on the emission properties of the LuAg:Ce single crystalline films and Su [6] on the optical properties of the U:CaF_2 crystals. The homogeneous dopant distribution in the laser materials is important because this affects the efficiency of the laser. There are a few reported results about the Pb^{2+} ions distribution in various crystals or on the segregation coefficient determination. Dmitriev [7] studied the influence of the Pb^{2+} ions on the optical properties of the TlBr crystal and determined the segregation coefficient; the reported values are 1.3–1.6. The distribution of trace amounts of metal impurities in CaF_2 crystals grown by the Bridgman method has been investigated by Yonezawa et al. [8]. They studied the distribution of both metal-fluoride and metal-oxide impurities in CaF_2 crystals obtained from highly pure fluoride powder. From their study it can be concluded that Li, Na and Pb hardly remain in CaF_2 crystals and the segregation coefficient is ≈ 1. The effective segregation coefficient of the Pb^{2+} ions in CaF_2 crystal was not reported yet.

The aim of this paper is to investigate the influence of PbF_2 content on optical properties of the CaF_2 crystals and to determine the effective segregation coefficient using the optical absorption method.

2. Experimental

Pure and PbF_2-doped CaF_2 crystals were grown in our crystal research laboratory using vertical Bridgman method. Suprapure grade (Merck) calcium fluoride and PbF_2 were used as the starting materials. It is known [8] that Pb^{2+} ions hardly remain in fluoride crystals if the usual Bridgman type technique is used for the growth of CaF_2 crystals. In order to obtain PbF_2-doped CaF_2 crystals the following procedure was used. First, pure, oxygen-free CaF_2 crystals were grown using the usual growth conditions, namely adding to the starting material an amount of 4 wt%PbF_2 as oxygen scavenger [9, 10]. The obtained CaF_2 crystals do not contain any undesired amount of lead ions or other impurities, as results from the optical absorption spectrum; then the PbF_2-doped crystals were grown from the crushed pure fluoride crystals doped with the desired amount of PbF_2. To prevent the evaporation of the PbF_2, a thin floating graphite lid was put on the charge in a sealed graphite crucible. In this work, four PbF_2-doped crystals have been investigated with the following amount of PbF_2 added in the starting mixture in the melt: 0.5, 1, 2, and 3 mol%PbF_2. Transparent colorless crystals of about 10 mm in diameter over 6–7 cm long were obtained in spectral pure graphite crucible in vacuum ($\approx 10^{-1}$ Pa) using a shaped graphite furnace [11]. The pulling rate was 4 mm/h. The crystals were cooled to room temperature using an estab-

* corresponding author; e-mail: nicoara@physics.uvt.ro

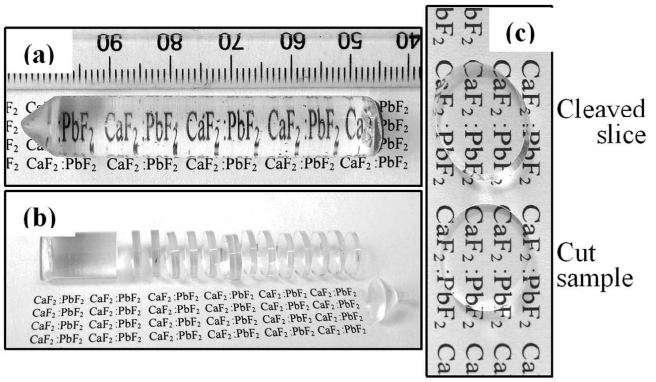

Fig. 1. As-grown x mol%PbF_2-doped CaF_2 crystals: (a) $x = 2$; (b) crystal cut for the distribution coefficient measurements, $x = 1$; (c) 1 mol%PbF_2 doped CaF_2 crystal-cleaved slice and $x = 0.5$ cut sample.

lished procedure. The as-grown single crystals are shown in Fig. 1.

The effective segregation coefficient, k_{eff}, has been determined using the optical absorption method [12–14]. In order to investigate the dopant concentration along the crystals and to determine the distribution coefficient, the crystals were cut from the bottom to the top into i = 14–15 slices (Fig. 1b). Each wafer was about 2 mm in thickness, and optically polished. The absorption coefficient $\alpha(i)$ of every slice was calculated from the absorption spectra for the well-shaped and strong characteristic absorption band of the Pb^{2+} ions, namely for $A = 306$ nm band. Taking into account the Beer–Lambert law, the absorption coefficient is proportional to the concentration, so the dopant distribution along the crystal can be estimated. The segregation coefficient for various PbF_2 concentrations in CaF_2 crystals was then calculated using a procedure described in Sect. 3.2. Room temperature optical absorption spectra were recorded by a Shimadzu 1650PC spectrophotometer.

3. Results and discussions

CaF_2 crystallizes in cubic structure with a typical fluorite lattice. In order to understand the optical properties and the dopant distribution in CaF_2 crystals it is better to see this structure as consisting of a simple cubic lattice of fluorine ions in which every other body center position is occupied by a Ca^{2+} ion. When various ions, such as alkaline metals, rare-earths or heavy metal ions, like Pb^{2+} are introduced into the lattice they usually occupy Ca^{2+} sites. If the introduced impurity ions have other valence than the Ca^{2+} ion, the valence mismatch is compensated in a variety of ways: by vacancy formation, by interstitial fluorine ion, etc. The Pb^{2+} ion has the same valence as Ca^{2+} but with a larger geometric size (0.143 nm) than the Ca^{2+} ion (0.126 nm), and for high dopant concentrations this will lead to distortion of the crystal lattice; this is the reason why the crystals doped with more than 3 mol%PbF_2 reveal structural defects, like blocks with different crystallographic orientations.

3.1. Optical absorption spectra

The presence of impurity ions in CaF_2 lattice with the ns^2 ground state configuration (like Pb^{2+} ions) induces absorption bands both in vacuum ultraviolet (VUV) and in UV domain [1, 2]. Four characteristic bands are located in UV domain, denoted by A, B, C, and D [1].

The absorption spectra of various concentrations CaF_2:PbF_2 samples reveal the four characteristic absorption bands of Pb^{2+} ions (Fig. 2).

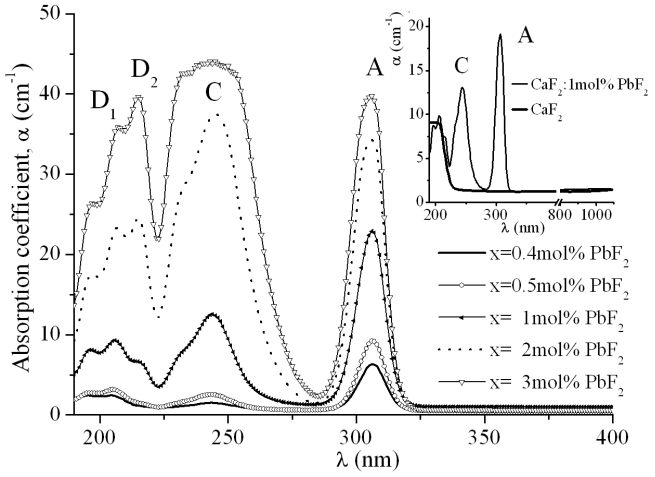

Fig. 2. Room temperature absorption spectra of PbF_2 doped CaF_2 crystals. The inset shows the absorption spectra of pure and 1 mol%PbF_2-doped CaF_2 crystals.

As Pb^{2+}-ions concentration increases, the shape of the C and D absorption bands modifies due to the overlap of many new bands that appear as a result of the energy levels splitting. Only the A band conserves ir sharp shape because no new components appear. This is the peak which we will use for the effective segregation coefficient determination by optical absorption method. The B band is observed only in the excitation spectra obtained for various bands of the emission spectra. For low concentrations (0.4 and 0.5 mol%PbF_2) only three peaks appear in the absorption spectrum: A = 306.2 nm, C = 243.1 nm and D = 203.7 nm; the A band is the strongest. For 1 mol% the following peaks are characteristic: A = 306.1 nm, the C band peaking at 244 nm for low concentration consists now of two overlapping bands peaking at 228 and 246 nm, as results from the excitation spectrum; the D band also splits into two bands: D_1 = 214 and D_2 = 206 nm. As the concentration increases, the peaks position are shifted to: A = 305.4 nm, C = 244 and 246 nm and a shoulder at 228 nm, $D_{1,2}$ = 215 and 206.8 nm for 2 mol%PbF_2. For 3 mol%PbF_2 sample the absorption bands are: A = 305.4 nm, C band becomes very broad as a result of an in-

crease in intensity of more than three overlapping components, and $D_1 = 215$, $D_2 = 207.5$ nm. The intensity ratio of the D band components differs for the samples with concentration $\geq$ 1 mol%PbF_2: the D_2 increases more than the D_1 component. The intensity of the D and C bands increases as the concentration increases and becomes comparable with the intensity of the A band.

Figure 3 shows the influence of the Pb^{2+} ions concentration (N_0) in the initial melt on the absorption coefficient of the A peak; the absorption coefficient was calculated for slices cut from the same position for every crystal. N_0 is the number of the Pb^{2+} ions per unit volume in PbF_2 doped CaF_2 crystals, calculated using the expression

$$N_0 = \rho \frac{C_L^0 N_A}{\mu}, \quad (1)$$

where ρ is the crystal density, C_L^0 is the dopant concentration (mol%) in the initial melt, N_A is Avogadro's number and μ is the molecular mass.

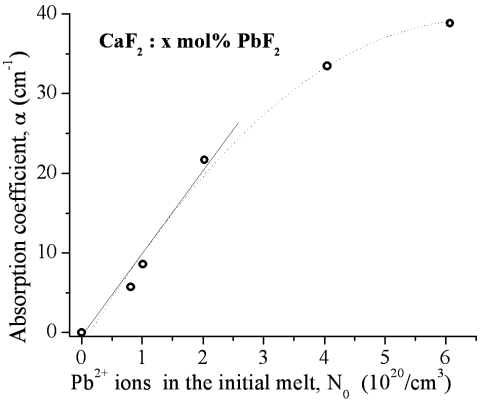

Fig. 3. Dependence of the absorption coefficient on the Pb^{2+} ions concentration (N_0) in the initial melt (measured for A band).

As the concentration increases, the absorption coefficient increases linearly for the first three concentrations: 0.4, 0.5 and 1 mol%PbF_2 (see Fig. 3), then a saturation behavior appears. The A peak shape, namely the absorption coefficient and the FWHM (the peak half-width), changes as the PbF_2 concentration increases, but no new components appear for this absorption band in comparison with C or D bands (see Fig. 2).

For a given PbF_2 concentration, the FWHM of the A peak is the same for the various slices cut along the crystal, only the absorption coefficient, α_i, varies from slice to slice, as is shown in Fig. 4. This behavior is used for the effective segregation coefficient determination by optical absorption method [12, 13].

The alkali halide crystals doped with ions which have the ns^2 electronic configuration in their ground state have been studied more extensively [1] than the alkaline-earth fluorides. The presence of this type impurity ion induces from three to six absorption bands in UV do-

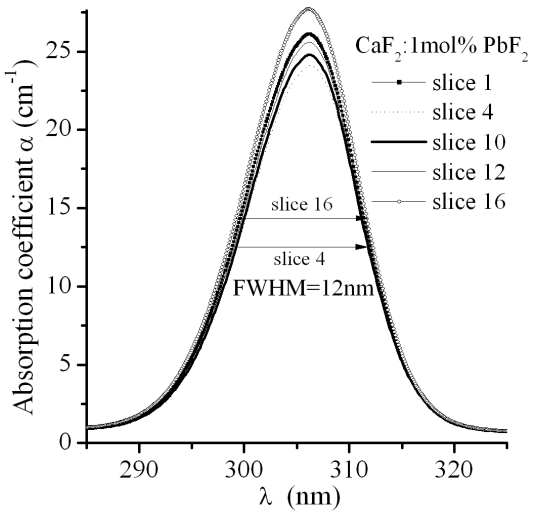

Fig. 4. The A band of various slices cut from 1 mol%PbF_2 doped CaF_2 crystal.

main. Oboth et al. [2] studied the absorption and emission spectra of Pb^{2+} centers in alkaline-earth fluorides in VUV domain, their A denoted absorption band corresponds to our D band.

The optical absorption bands are assigned to electronic transitions from the $(6s^2)$ ground state to the $(6s^1)$ $(6p^1)$ excited state: A ($^1S_0$–$^3P_1$, spin orbit allowed), B ($^1S_0$–$^3P_2$ vibrationally allowed), and C ($^1S_0$–$^1P_1$ dipole allowed).

3.2. Determination of the effective segregation coefficient of Pb^{2+} ions

The effective segregation coefficient (k_{eff}) at a given growth rate is defined by

$$k_{\text{eff}} = C_S / C_L^0, \quad (2)$$

where C_S is the dopant concentration at the bottom of the as-grown crystal and C_L^0 is the dopant concentration in the initial melt. The value of C_S can be measured by various methods, or estimated from optical absorption measurements [12–14].

The effective segregation coefficient determination of the Pb^{2+} ions in CaF_2 host by optical absorption method is based on the following two laws.

(a) According to the Beer–Lambert law the absorption coefficient is proportional to the sample concentration (C), $\alpha = aC$, where a is the absorption coefficient for unit Pb concentration and unit light path length; a may be recognized as constant for the investigated Pb^{2+} ions concentration [12–14]. The Pb^{2+} ions concentration can be estimated from the measured optical density, O.D. $= \log(I_0 R/I)$, where I_0 is the light intensity incident on the sample, R is the the reflection factor on sample surface, I is the transmitted light intensity [13]. Taking into account the relation

$$I = I_0 R \exp(-\alpha d), \quad (3)$$

where α is the absorption coefficient and d is the sample

thickness, the dopant concentration of a slice can be estimated using the relation [13]:

$$C = \frac{\alpha}{a} = \frac{2.30258 \text{ O.D.}}{ad} . \quad (4)$$

(b) The dopant concentration (along the growth axis) at the distance z from the origin of the crystal can be obtained by using the classical relation [15]:

$$C_{\mathrm{S}}(z) = C_{\mathrm{L}}^{0} k_{\mathrm{eff}} \left[1 - g(z)\right]^{k_{\mathrm{eff}}-1} , \quad (5)$$

where $g(z)$ is the crystallized fraction of the melt given by $g(z) = V_p\ t/L = z/L$, V_p is the crystal growth rate, t is the growth time and L is the crystal length, so $V_p t$ is the grown crystal length, z, at the moment t. The more the k_{eff} differs from unity, the larger is the concentration gradient in the crystal.

Therefore, taking into account the Beer–Lambert law, the dopant distribution along the crystal length can be estimated using the optical absorption method. In order to determine the effective segregation coefficient, we cut the crystal into i slices with the same thickness (Fig. 1b) and calculate the absorption coefficient for the absorption peak at 306 nm, from the optical absorption spectrum of every slices ($\alpha(z)$). Using the relations (4) and (5), the following expression is obtained in order to determine the effective segregation coefficient:

$$\log \alpha(z) = (k_{\mathrm{eff}} - 1) \log (1 - z/L) + \log \left(a k_{\mathrm{eff}} C_{\mathrm{L}}^{0}\right) . (6)$$

The effective segregation coefficient can be calculated from the slope $m = k_{\mathrm{eff}} - 1$, of the fitting line of $\log\ \alpha(z)$ versus $\log(1 - z/L)$.

Figure 5 shows the Pb^{2+} ions distribution (characterized by the absorption coefficient) along the four investigated crystals, with various PbF_2 concentrations in the initial melt. The dopant distribution along the crystals shows some oscillations of the Pb^{2+}-ions concentration. These types of oscillations have been also observed for other crystals grown by the Bridgman technique; this behavior has not been explained yet [16, 17]. For concentrations ≤ 1 mol% the absorption coefficient increases along the crystals and consequently, the concentration increases, too. For CaF_2:2 mol%PbF_2 sample the dopant distribution along the crystal has the strongest oscillatory behavior; for the 3 mol%PbF_2–CaF_2 sample the absorption coefficient decreases along the crystal (the concentration also decreases).

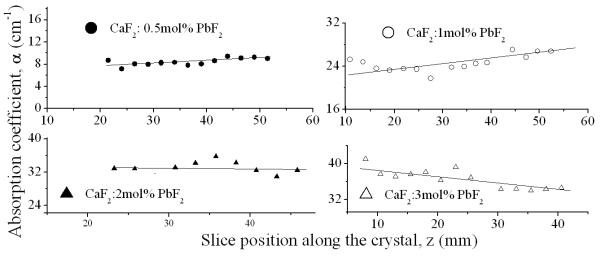

Fig. 5. Pb^{2+} ions distribution along the crystals characterized by the absorption coefficient; the PbF_2 concentration in the initial melt is indicated in the figure.

TABLE

Effective segregation coefficient.

CaF_2: x mol%PbF_2	$x = 0.5$	$x = 1$	$x = 2$	$x = 3$
k_{eff}	0.85	0.925	1.002	1.15

The calculated effective segregation coefficient for the studied samples is shown in Figs. 6, 7 and Table. As the concentration of the Pb^{2+} ions in the initial melt increases, the effective segregation coefficient, k_{eff}, increases, too. The obtained values are: 0.85 for CaF_2:0.5 mol%PbF_2 crystal, 0.925 for CaF_2:1 mol%PbF_2 crystal, 1.002 for CaF_2:2 mol%PbF_2 crystal and 1.15 for CaF_2:3 mol%PbF_2 crystal.

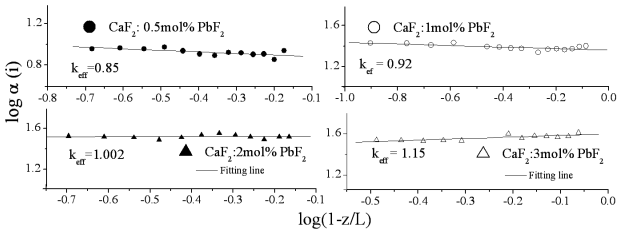

Fig. 6. Fitting lines of $\log \alpha(z)$ vs. $\log(1 - g)$ in order to calculate the effective segregation coefficient; the obtained k values are indicated in the figures.

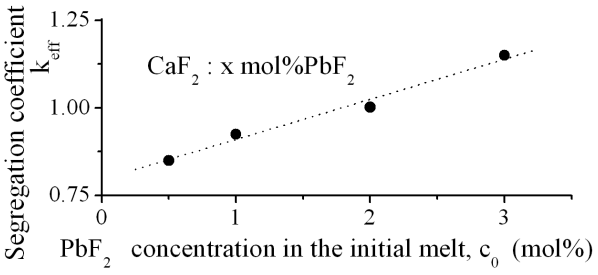

Fig. 7. Dependence of the effective segregation coefficient of Pb^{2+} ions in CaF_2 on the PbF_2 concentration in the initial melt.

Preliminary luminescence studies reveal a strong emission spectrum in the near UV domain (at 323 nm and 341 nm) and in the visible region (at 644 nm). The strongest emission has been obtained for CaF_2:2 mol%PbF_2 probe. Because the effective segregation coefficients are almost equal to unity, the Pb^{2+}-ions distribution in CaF_2 crystals is approximately uniform and from this point of view, PbF_2-doped CaF_2 crystals could be a good laser material in near UV domain.

4. Conclusions

Various PbF_2 concentrations doped CaF_2 crystals were grown using the conventional Bridgman technique. In

order to prevent the PbF_2 evaporation a special crystal growth procedure was adopted. The absorption spectra reveal the characteristic absorption bands of the Pb^{2+} ions. A strong concentration dependence of the absorption spectra has been observed. The effective segregation coefficient of the Pb^{2+} ions in CaF_2 host has been determined using the optical absorption method. The segregation coefficient of Pb^{2+} ions in CaF_2 has not been reported before.

Acknowledgments

This work was supported by the Science Research Council, Romania, grant CEEX no. 72/2006.

References

[1] P.W.M. Jacobs, *J. Phys. Chem. Solids* **52**, 35 (1991).

[2] K.P. Oboth, F.J. Lohmeller, F. Fischer, *Phys. Status Solidi B* **154**, 789 (1989).

[3] M. Fockele, F. Lohse, J.-M. Spaeth, R.H. Bartram, *J. Phys., Condens. Matter* **1**, 13 (1989).

[4] R.H. Bartram, M. Fockele, F. Lohse, J.-M. Spaeth, *J. Phys., Condens. Matter* **1**, 27 (1989).

[5] V. Babin, V. Gorbenko, A. Makhov, M. Nikl, S. Zazubovich, Y. Zorenko, *Phys. Status Solidi C* **4**, 797 (2007).

[6] L. Su, W. Yang, J. Xu, Y. Doung, G. Zhou, *J. Cryst. Growth* **270**, 150 (2004).

[7] Y. Dmitriev, P.R. Bennett, L.J. Cirignano, T.K. Gupta, W.M. Higgins, K.S. Shah, P. Wong, *Nucl. Instrum. Methods Phys. Res. A* **578**, 510 (2007).

[8] T. Yonezawa, J. Nakayama, K. Tsukuma, Y. Kawamoto, *J. Cryst. Growth* **244**, 63 (2002).

[9] D.C. Stockbarger, *J. Opt. Soc. Am.* **39**, 731 (1949).

[10] A. Molchanov, J. Friedrich, G. Wehrhan, G. Muller, *J. Cryst. Growth* **273**, 629 (2005).

[11] D. Nicoara, I. Nicoara, *Mater. Sci. Eng. A* **102**, L1 (1988).

[12] K. Shiroki, Y. Kwan, *J. Chem. Soc. Japan* **7**, 940 (1978).

[13] Y. Kuwano, *J. Cryst. Growth* **57**, 353 (1982).

[14] D. Sun, Q. Zhang, Z. Wang, J. Su, C. Go, A. Wang, S. Yin, *Cryst. Res. Technol.* **40**, 698 (2005).

[15] D.T. Hurle, *Crystal Pulling from the Melt*, Springer-Verlag, Berlin 1993.

[16] C. Barat, Ph.D. Thesis, University of Rennes, 1995.

[17] A. Mitric, T. Duffar, C. Diaz-Guerra, V. Corregidor, L.C. Alves, C. Garnier, G. Vian, *J. Cryst. Growth* **287**, 224 (2006).